Computer Assisted Methods in Engineering and Science, **26**: 137–151, 2019, doi: 10.24423/cames.269

Experimental verification of a numerical model of RC beam with CFRP rope strengthening

Michał Szczecina*, Paweł Tworzewski, Kamil Bacharz

Kielce University of Technology
Department of Civil Engineering and Architecture
al. 1000-lecia Państwa Polskiego 7, 25-314 Kielce, Poland
**Corresponding Author e-mail: michalsz@tu.kielce.pl*

This paper presents results of experimental tests and numerical analysis of reinforced concrete (RC) beams containing an additional carbon fibre rope strengthening. Two single-span RC beam specimens with classical reinforcing bars and stirrups and one carbon fibre rope as near-surface mounted (NSM) strengthening were tested in a four-point bending test. The paper presents and compares the results registered by the ARAMIS system during the test of two beams with carbon fibre rope under monotonic load with the results obtained in finite element analysis with Abaqus software using the concrete damaged plasticity model for concrete.

Keywords: RC beams, CFRP strengthening, FEM, Abaqus, CDP model.

1. Introduction

The strengthening of existing building structures is often related to their rebuilding or changes in their purpose. This has also become the reason for the emergence of a number of different construction and material solutions over the years. The basic strengthening methods of RC structures were: increasing the cross-section dimensions by concreting the compression zone, increasing the reinforcement amount in the tensile zone, or changing the static scheme [1]. Currently, the most common form of strengthening beams and other elements is the use of composite fibre (FRP): aramid (AFRP), glass (GFRP), basalt (BFRP), and carbon fibre (CFRP) – very popular because of their modulus of elasticity. However, the use of additional materials in the form of various types of fibres results in more and more complex calculation systems, which due to their complexity have contributed to the creation of many scientific works in various research centres (including national) [2–4]. It should also be noted that the use of the indicated polymeric materials is also associated with the appropriate application technology. As a result, we can distinguish: application system on the external surface of the strengthened element (externally bonded – EB), application in the form of pasting to pre-prepared groove in the surface of the strengthened element (NSM) or strengthening connected to the substrate using glue and anchors or only anchors (mechanically anchored – MA). In addition, the passive and active reinforcement system can also be distinguished, where the composite is prestressed [5, 6]. The previously mentioned anchoring is also performed in the case of mats with, for example, ropes. One of the methods of such fixing is the use of the SikaWrap FX-50C [7] composite rope, which can also be used as an autonomous strengthening system for RC elements. In addition, such ropes are characterised by large freedom in shaping the trajectory of the reinforcement (as opposed to composite laminates) and enable the execution of a single anchorage, without the need for external anchors. For this reason, a composite rope (SikaWrap FX-50C) was used as the main reinforcement for RC beams. The aim of the paper was to compare the results of the experimental RC beam strengthened with a composite rope with numerical analysis carried

out in the Abaqus program, and also verify the possibility of creating a numerical model simulating the real work of the element.

2. Tested elements and description of experimental studies

The results refer to the examination of two single-span RC beams with a total length of 3.3 m (distance between supports' axes: 3.0 m) and a rectangular section with dimensions of 0.3×0.12 m. In the beams, two reinforcing bars with the diameter of ∅14 were used as the bottom reinforcement and two ∅8 as the upper reinforcement. The reinforcement ratio with steel bars was $\rho_s = 0.93\%$. The beams were made in a concrete precast factory with a planned class of concrete C40/50 and steel B500SP. During the concreting, the cube shape samples were taken: $150 \times 150 \times 150$. The elements were strengthened by using a SikaWrap FX-50C composite rope. To increase the effectiveness, the composite reinforcement was embedded in epoxy resin in pre-cut grooves in a concrete cover (NSM reinforcement). In order to ensure proper anchorage, the end of the rope was put into the vertical holes made in the support zones (Fig. 1). The carbon fibres were impregnated over the entire length with Sikadur-300 resin. The Sikadur-330 resin was used to fill pre-cut grooves (width 1 cm, depth 2 cm) and drilled holes (diameter 2 cm). The obtained composite reinforcement ratio was $\rho_f = 0.8\%$.

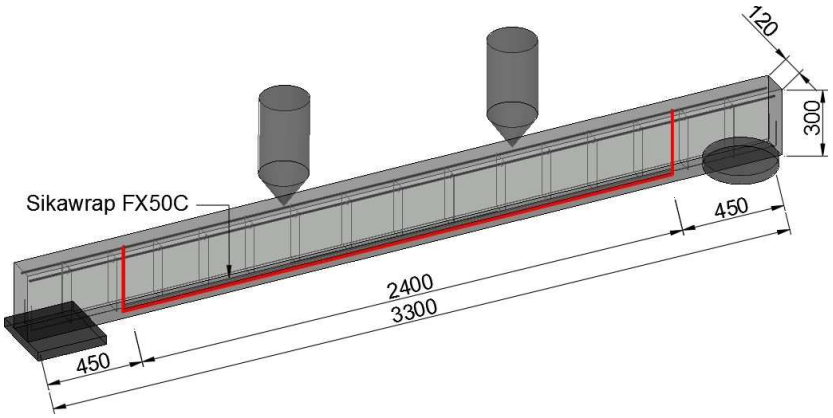

Fig. 1. Beam strengthening scheme.

The measurements of strains on the side surface, the crack width and displacements were carried out by the ARAMIS system. Two sensors were used for registration (area measured with two sensors showed in Fig. 2).

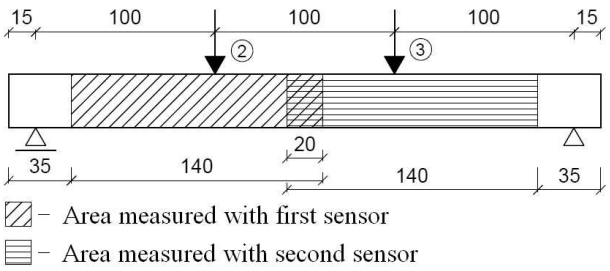

Fig. 2. Static scheme.

The deflection was also measured with the use of five inductive sensors. The beams were loaded monotonically until failure with two concentrated forces, as it is shown in Fig. 3.

The ARAMIS optical measuring system uses a digital image correlation method. The device used in studies was equipped with a monochrome Baumer TXG50 cameras with a resolution of

a)

b)

Fig. 3. Test stand: a) front, b) back.

2448×2050 pixels and Schneider Kreuznach Cinegon 1.4/12-0906 lenses [8] (Fig. 4). This kit allows recording up to 15 images per second with full resolution. The use of the ARAMIS optical measuring system in RC element studies enables observing the cracks' development process, tracking changes in the position of points. This allows 3D measurement of spatial displacement, for any point located in the test area, recorded by the camera and tracking strains on the entire surface of the element during loading.

Fig. 4. Aramis system (digital image correlation).

To determine the strength properties for materials used to prepare those elements, a compressive strength test of concrete cubes and tensile test for steel bars were carried out. The results are shown in Table 1.

Table 1. The results of testing the parameters of concrete and steel.

Compressive strength test of concrete cubes		
	Date of concreting/test date:	14.07.2017/ 28.02.2018
Samples: $0.15 \times 0.15 \times 0.15$ mm	$f_{cm,\mathrm{cube}}$ =	76.8 [MPa]
	s =	2.8 [MPa]
Number of samples: 12	ν =	3.7%
	f_{cm} =	61.4 [MPa]
Tensile test for steel bars		
Samples: ∅14	$R_{p0.2}$ =	505.8 [MPa]
	s =	5.8 [MPa]
Number of samples: 42	ν =	1.13%
	E =	219.8 [GPa]

For both beams, the failure mode was the same – breaking of the composite reinforcement under the load point, close to the sliding support (Fig. 5).

Fig. 5. Rupture of the composite material.

3. Numerical model

The numerical analysis was performed using Abaqus software, ver. 6-12.2. In this chapter, material models for concrete and steel used in the research are described. There is also a description of finite element (FE) model features, including material constants, meshing, boundary conditions, loading regime, model parameters, solution procedure, etc. The following chapter presents the results of FE calculations.

3.1. Material model of concrete

In order to consider a non-linear, post-peak behaviour of concrete, the so-called Barcelona model [9, 10] was applied for concrete. In Abaqus software, it is known as "concrete damaged plasticity"

(CDP). The model is a combination of plasticity theory and damage mechanics and introduces the so-called damage parameters, separately d_t for tension and d_c for compression, which are used to define the damage parameter d according to the equation:

$$1 - d = (1 - d_c s_t)\,(1 - d_t s_c)\,, \tag{1}$$

where s_t and s_c are stiffness recovery functions. Then, the constitutive equation can be defined as:

$$\sigma = (1 - d)\,\mathbf{D}_{\mathbf{o}}^{\mathbf{el}} : \left(\boldsymbol{\varepsilon} - \boldsymbol{\varepsilon}_{\mathbf{pl}}\right), \tag{2}$$

where σ and ε denote stress and strain tensor, $\mathbf{D}_{\mathbf{o}}^{\mathbf{el}}$ is an initial stiffness matrix in the elastic state, and a colon stands for a scalar product of tensors. The yield function used in CDP is presented in the plane stress state in Fig. 6.

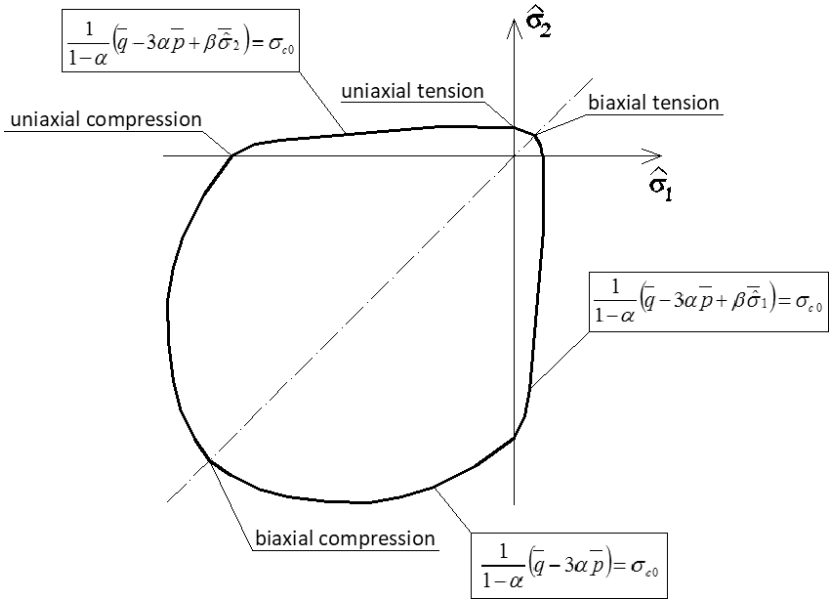

Fig. 6. The yield function in the plane stress state [11].

The potential plastic flow is assumed as non-associated, and the flow potential G is the hyperbolic function whose graph in the meridian plane is presented in Fig. 7.

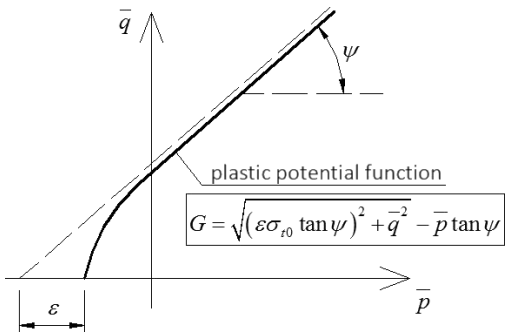

Fig. 7. The flow potential function in the meridian plane [11].

The graph also presents a geometric interpretation of two important CDP model parameters, namely dilation angle ψ and eccentricity ε. The eccentricity parameter ε is often assumed as equal to 0.1 according to [11], but the value of the dilation angle requires a proper calibration. Some work

in this subject was done and presented in [12]. The suggested value of the dilation angle should be in an interval from 5 to 15.

It is also possible to apply the viscoplastic regularization to the CDP model, according to [13]. The rate of change of viscoplastic strains can be derived according to the equation:

$$\dot{\varepsilon}_v^{pl} = \frac{1}{\mu}\left(\varepsilon^{pl} - \varepsilon_v^{pl}\right), \tag{3}$$

where differentiation is in the time domain, superscript pl stands for plastic part of strains, subscript ν means viscous strains, and μ denotes a relaxation time. The relaxation time is called "viscous parameter" in Abaqus code, and also requires a proper calibration. According to [12], the relaxation time should be a relatively small number, e.g., 10^{-4} s if a loading time (or strictly a load parameter in static analysis) is assumed as 1 s.

A uniaxial compressive behaviour of concrete can be defined in Abaqus by giving a set of points lying on the $\sigma - \varepsilon$ curve. For the uniaxial tension behaviour of concrete, there are three ways to define it, namely inputting:

- a set of points laying on the $\sigma - \varepsilon$ curve,
- a set of points laying on the $\sigma - u_{cr}$ curve, where u_{cr} denotes a crack width,
- a fracture energy of concrete G_f.

If one uses advanced concrete models in FEM, some numerical problems are likely to occur when solving FEM equations. One of these problems is mesh sensitivity. To avoid such a problem, it is advised to use the so-called "fracture energy trick" [14]. This means that the use of fracture energy to model the tension behavior of concrete can be preferable. The reason is that thanks to the given value of G_f FEM program can derive a value of u_{cr} for each finite element separately. A geometrical interpretation of the fracture energy is presented in Fig. 8, where σ_1 is stress in uniaxial tension.

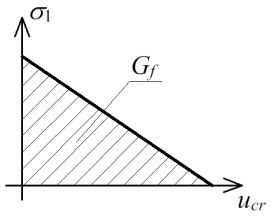

Fig. 8. The constitutive relationship for reinforcing steel [11].

A CDP model for concrete is a very robust and popular model chosen by users of Abaqus software, but it also requires very precise calibration of its parameters, especially dilation angle and relaxation time. Some work on CDP model properties and calibration of its parameters was presented in [15–18].

3.2. Material model of reinforcing steel

A classical von Mises yield criterion [11] was used to model behaviour of reinforcing steel in Abaqus. An elastic-ideally-plastic model shown in Fig. 9 was assumed to define the constitutive relationship for reinforcing steel [19].

3.3. Properties of specimen for FEM calculations

The FEM analysis was performed in 3D state using C3D8R solid finite elements – eight-node linear bricks with reduced integration and enhanced hourglass control. This kind of finite element was

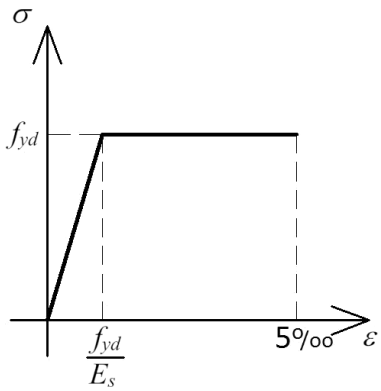

Fig. 9. The constitutive relationship for reinforcing steel [3].

applied to all components of the beam – concrete matrix, reinforcing steel and reinforcing FRP rods. A general view of the meshed specimen, boundary conditions and loads, and a view of all components and global coordinate system are presented in Figs 10 and 11, respectively. The average size of a finite element for a concrete beam was assumed as 20 mm.

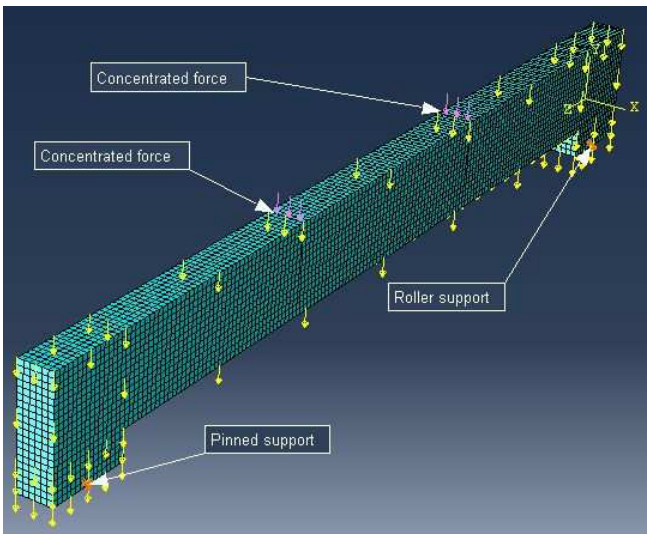

Fig. 10. 3D view of the meshed specimen.

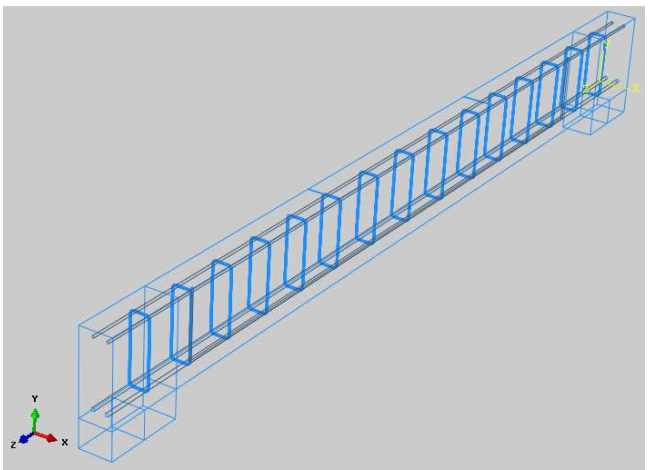

Fig. 11. 3D view of a concrete beam and reinforcement.

The CDP model for concrete and the classical metal plasticity for reinforcing steel were applied. Input variables of the CDP model were as follows: concrete C55/67, elastic modulus E_{cm} = 38 GPa, Poisson's ratio ν = 0.2, tension strength f_{ctm} = 4.2 MPa, compression strength f_{cm} = 63 MPa, fracture energy G_f = 153.9 Nm^{-1}, dilation angle 15 degrees, relaxation time 1 s, $\sigma - \varepsilon$ relationship (compressive behaviour of concrete) according to Eurocode [19] for non-linear analysis. Some other parameters were assumed as default according to Abaqus manual [11], namely: flow potential eccentricity 0.1, the ratio K of the second stress invariant on the tensile meridian to that on the compressive meridian for the yield function equal to 0.667, and the ratio f_{b0}/f_{c0} of biaxial compressive yield stress to uniaxial compressive yield stress equal to 1.16. Mechanical properties of reinforcing steel were based on the uniaxial tension test separately for each rebar diameter and were applied as follows:

- for 6 mm rebars – E_s = 213 GPa, f_y = 590 MPa,
- for 8 mm rebars – E_s = 217 GPa, f_y = 583 MPa,
- for 14 mm rebars – E_s = 220 GPa, f_y = 506 MPa.

Poisson's ratio of reinforcing steel was assumed as ν = 0.3.

The carbon fibre rope [7] was modelled using a linear constitutive relationship and the elasticity theory. Such a choice of a material model results from the relatively high value of fibre tensile strength, namely 4 GPa. Elasticity modulus was assumed as 240 GPa and Poisson's ratio ν = 0.25. A cross-section area of the rope was 28 mm^2.

A constraint for all components was applied as an "embedded region", which means a full-bond between concrete matrix and reinforcement, both steel rebars and CFRP rope.

A dead load and two concentrated forces exerted by hydraulic cylinders were applied to the beam. The loading time was assumed according to the laboratory tests, namely: 10 022 s for the BW-12-M1 specimen and 9960 s for the BW-12-M2 specimen. Maximum values of concentrated forces were assumed as 55.5 kN for BW-12-M1 and 54.9 kN for BW-12-M2. The solution of non-linear FE problem was performed in Abaqus/Standard using direct, full-Newton incremental procedure, where an initial increment was assumed as 10 s, maximum was equal to 100 s and minimal to 10^{-6} s.

4. Results of numerical analysis

In this chapter, the following chosen results of FE analysis are presented:

- a nodal vertical displacement compared with the test results,
- crack pattern compared with the results from the ARAMIS system and crack width,
- stress and yielding in reinforcing steel and fibre rope.

The following output variables available in Abaqus post-processor are presented in this chapter:

- PEEQT – equivalent plastic strain in tension, which is also used to calculate a crack width,
- AC YIELD – yielding of reinforcing steel; the variable has two values only: 1 means yielding and 0 denotes no yielding of reinforcing steel,
- S, Mises – von Mises equivalent stress.

The crack width w was calculated according to the formula given by Červenka *et al.* [20]:

$$w = \varepsilon_{cr}\left(1 + (\gamma_{\max} - 1) \cdot \frac{\theta}{45}\right) L_t, \tag{4}$$

where ε_{cr} denotes equivalent plastic strain in tension, θ is an angle between the vertical axis of a global coordinate system and a direction of the crack propagation, and L_t stands for a length of a finite element perpendicular to the direction of the crack. A default value of $\gamma_{\max}$ is 1.5 [20].

4.1. Results for the BW-12-M1 specimen

The results of FE analysis for the BW-12-M1 specimen are presented in Figs 12–16. For the sake of better visibility of stress and strain maps, some results are presented for half of a specimen, as for the rest of the model, the results are approximately symmetric. The maximum stress in the fibre rope is about 3.27 GPa, which is lower than the assumed tensile strength of the rope, so in the numerical analysis the rope did not break off. The bottom reinforcement yielded in the middle of the beam and the stirrups did not undergo any yield. The crack propagation seems to be quite similar in the laboratory test and Abaqus, though, in the last increment, there is a clear

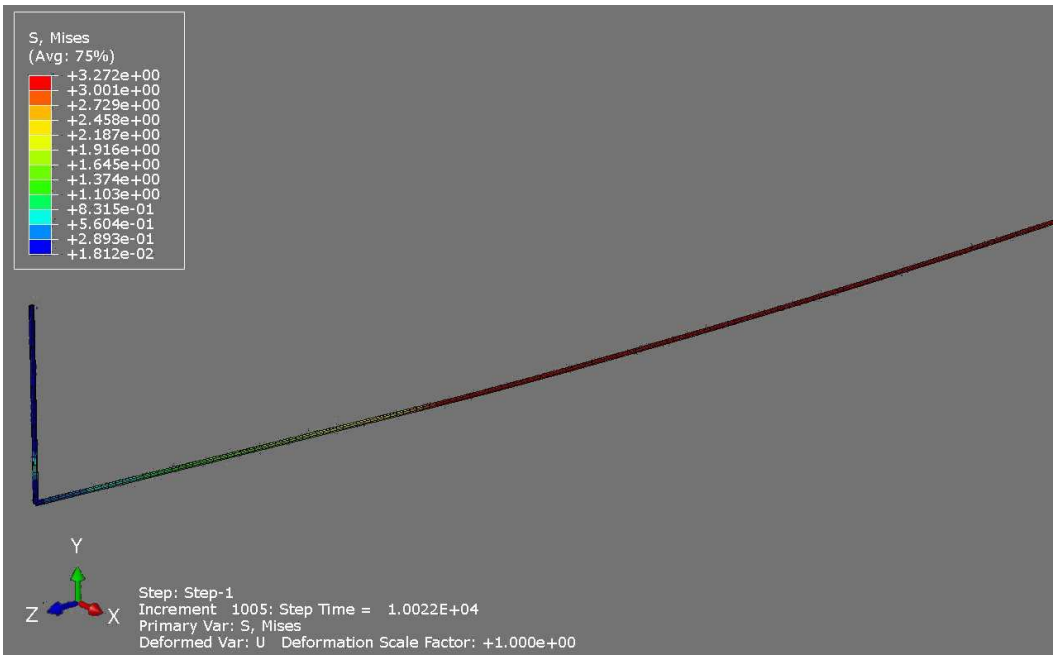

Fig. 12. The von Mises equivalent stress [GPa] in the carbon fibre rope (partial view).

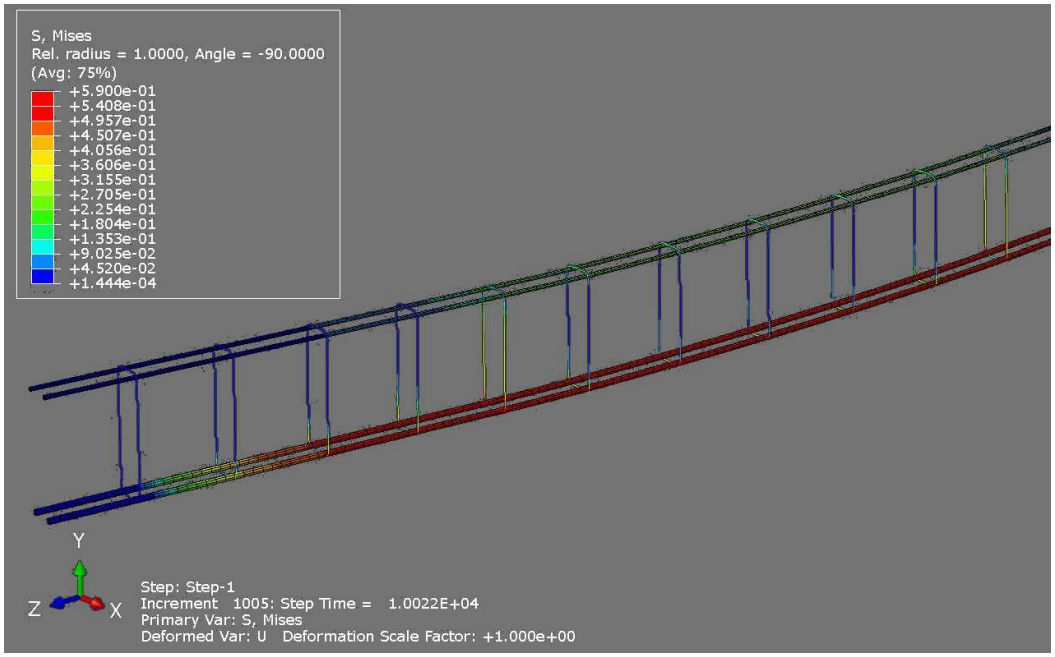

Fig. 13. The von Mises equivalent stress [GPa] in the reinforcing steel (partial view).

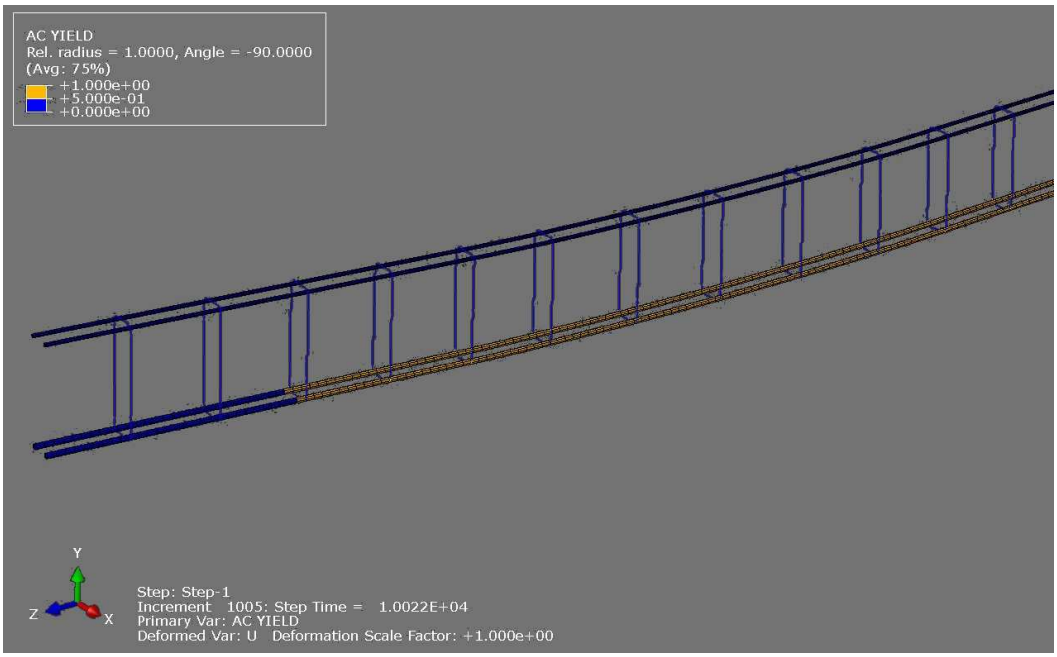

Fig. 14. Yielding of the reinforcing steel, yellow colour means full yielding (partial view).

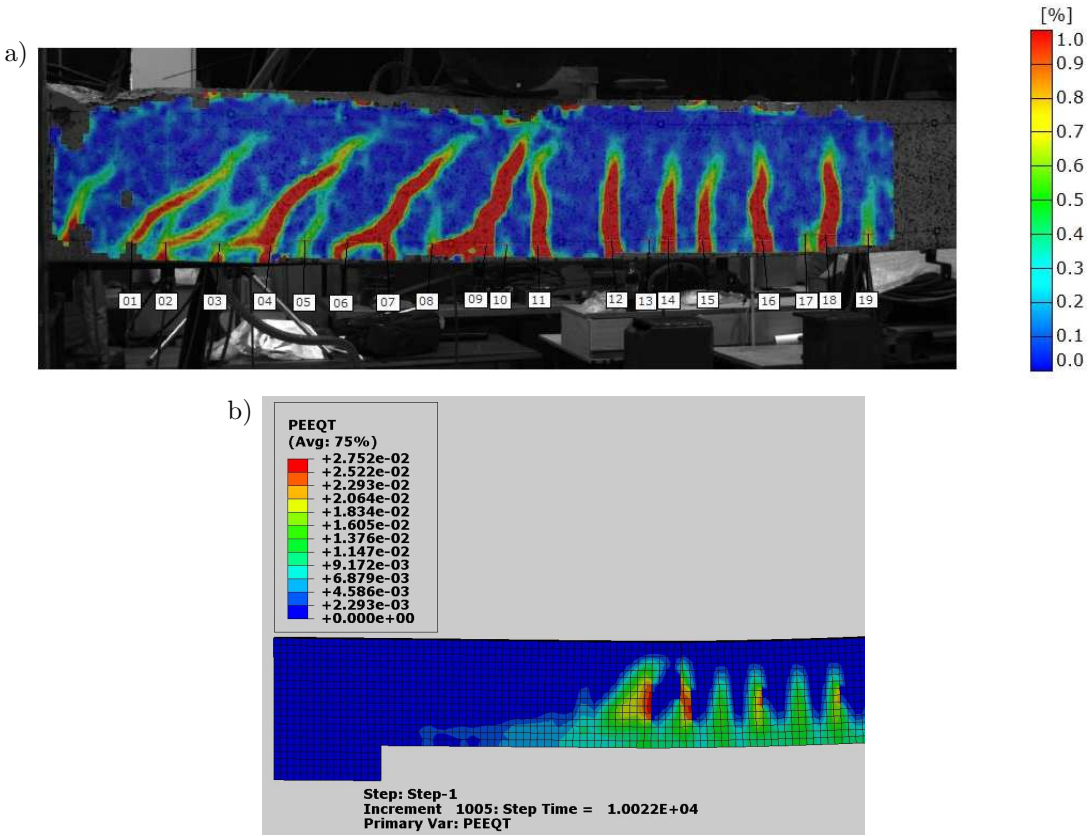

Fig. 15. PEEQT in the last increment obtained in the laboratory test (ARAMIS) (a) and in Abaqus (partial view) (b).

localization of the maximum PEEQT strain under a hydraulic cylinder. The numerical model did not reproduce all the diagonal cracks in the support zone but reproduced well vertical cracks in the

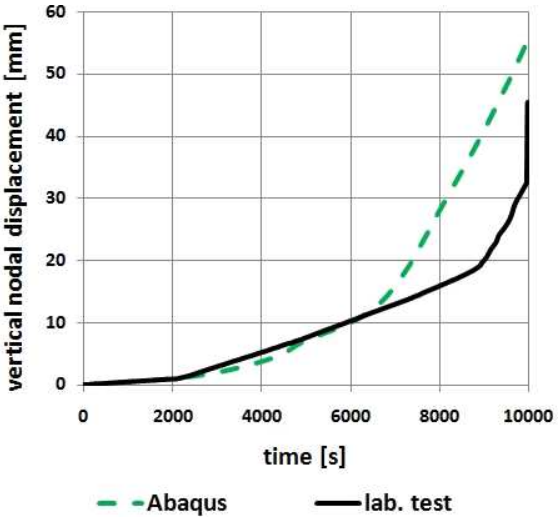

Fig. 16. The vertical nodal displacement in the middle of the beam.

middle of the beam. The maximum crack width in the last increment in Abaqus was calculated as 0.55 mm. It was also possible to establish the increment in which the crack is equal to 0.30 mm – that was in time point $t = 6703$ s, which corresponds to the concentrated force 36.7 kN. In Fig. 11, there is presented a relationship of a vertical nodal displacement vs time obtained in the test and Abaqus. Till the time point circa $t = 6000$ s, both graphs actually coincide, but then the response in the laboratory test is stiffer. The maximum deflexion obtained was Abaqus is higher and it was 56 mm, while in the laboratory test it was around 45 mm.

4.2. Results for the BW-12-M2 specimen

The results obtained for the BW-12-M2 specimen did not significantly varied from those presented in the previous subchapter. All the results are presented in Figs 17–21. The maximum stress in

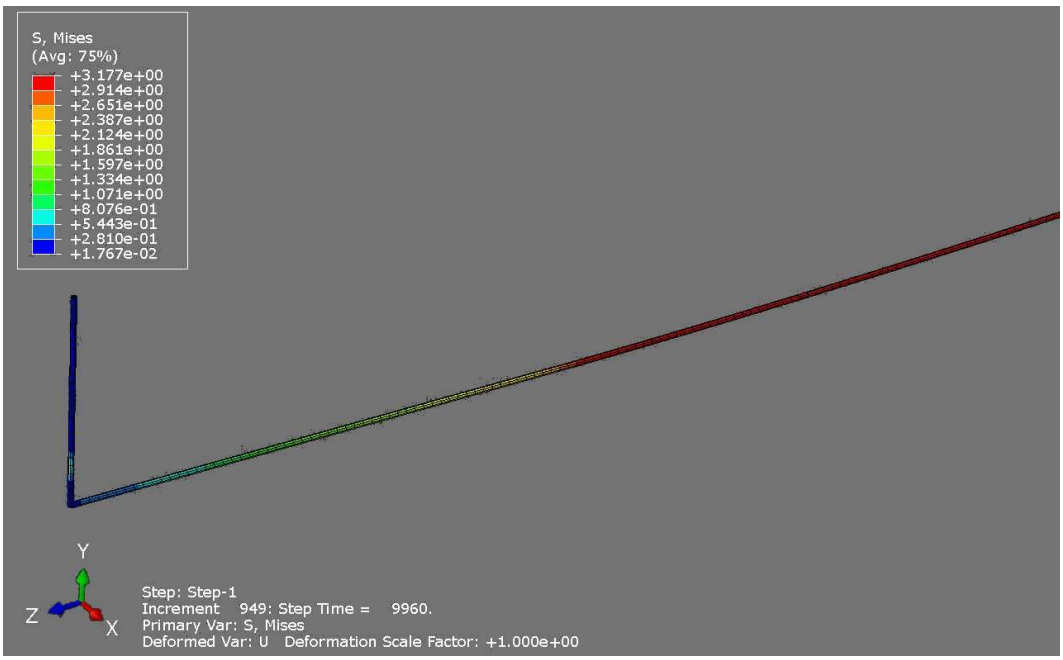

Fig. 17. The von Mises equivalent stress [GPa] in the carbon fibre rope (partial view).

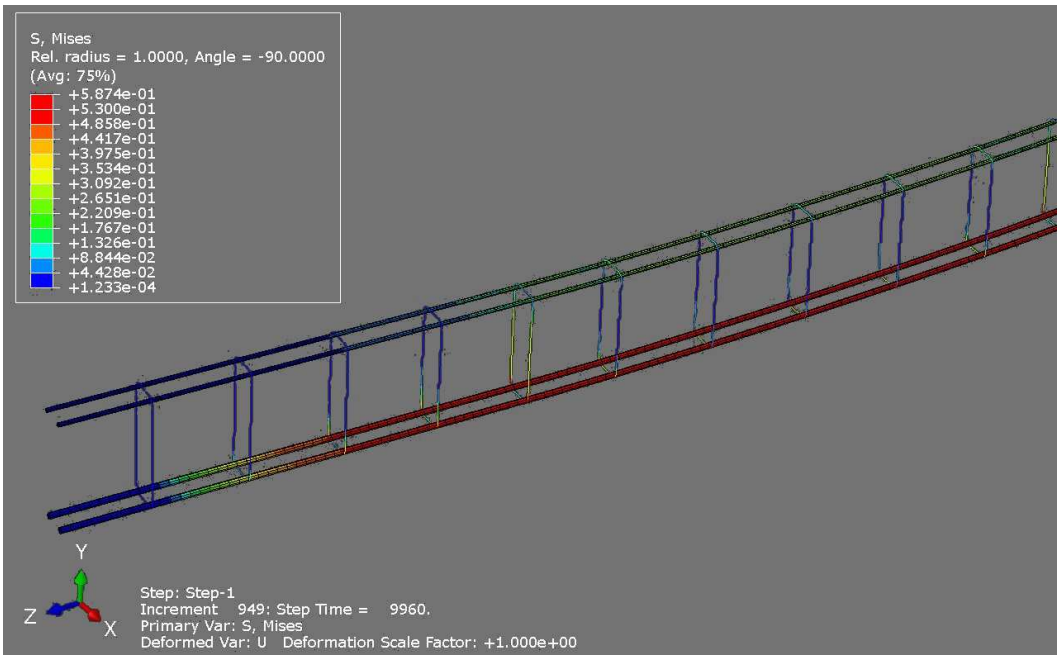

Fig. 18. The von Mises equivalent stress [GPa] in the reinforcing steel (partial view).

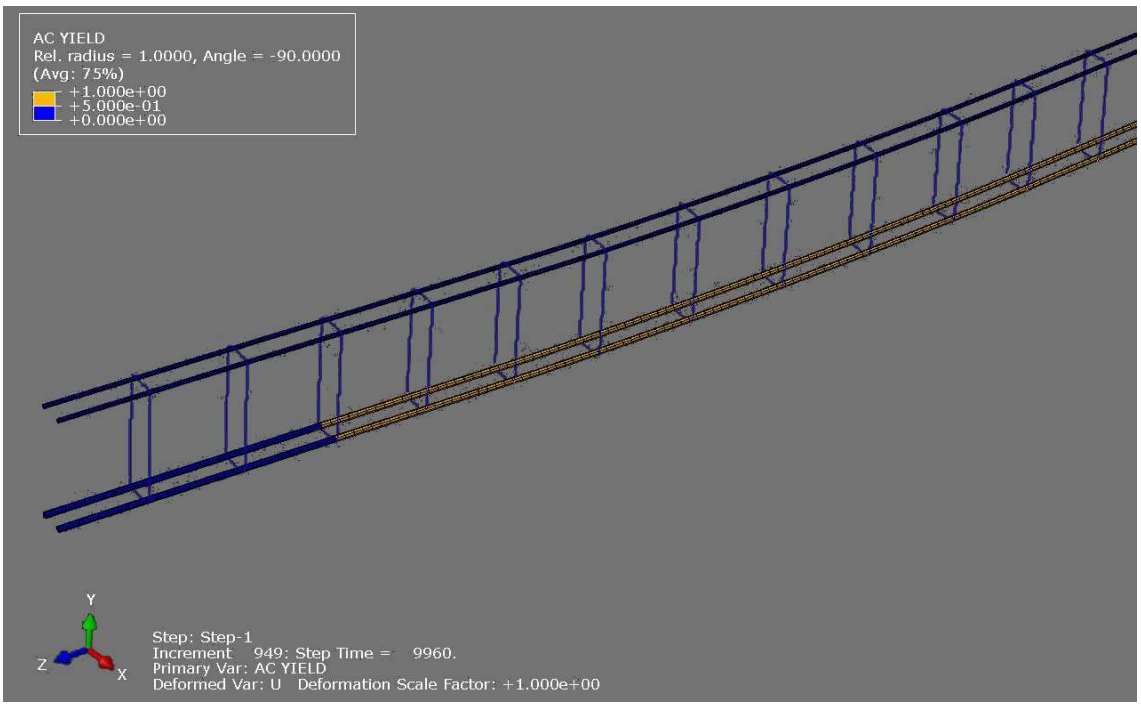

Fig. 19. Yielding of the reinforcing steel, yellow colour means full yielding (partial view).

the fibre rope was 3.18 GPa, which was still lower than the tensile strength of the rope. The crack pattern was similar to that obtained in the laboratory test but did not reproduce the diagonal cracks in the support zone. The maximum crack width was 0.57 mm, while crack width equal to 0.30 mm was obtained for the concentrated force equal to 37.4 kN and time point $t = 6709$ s. After exceeding time $t = 6000$ s, again the response of the specimen was stiffer in the laboratory test. The maximum deflexion obtained in Abaqus was higher and it was 54 mm, while in the laboratory test it was around 36 mm.

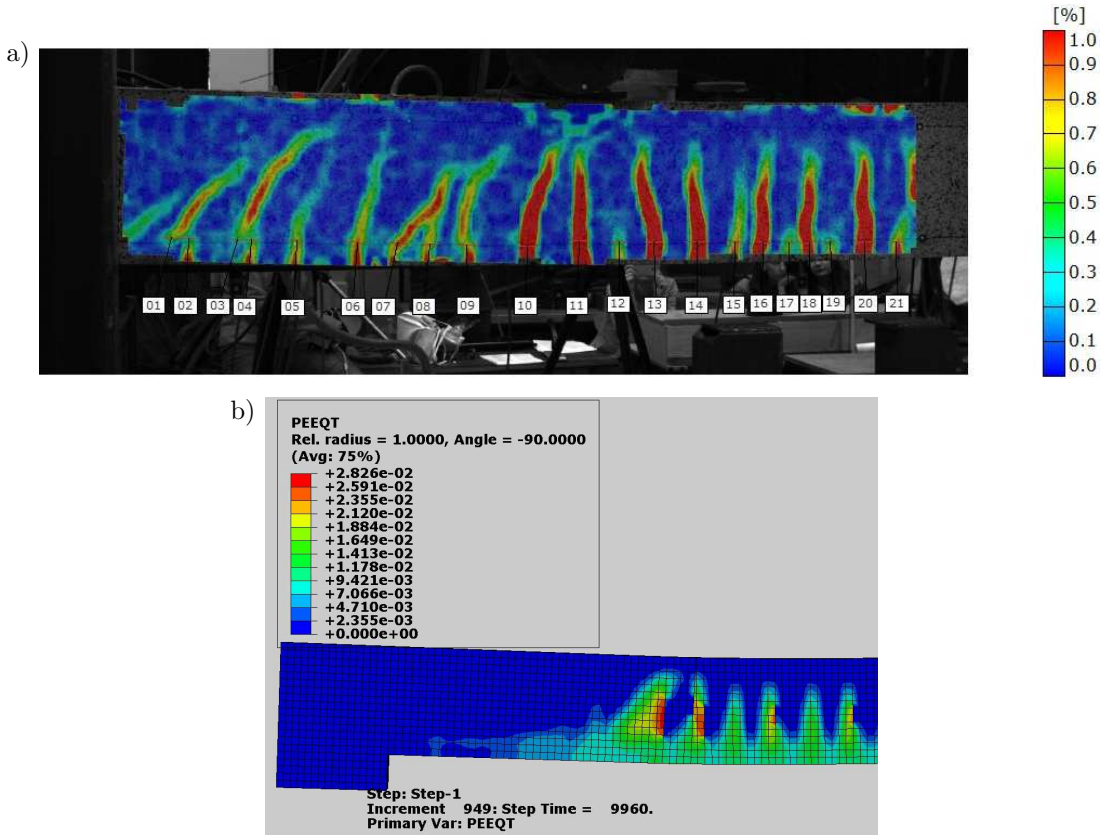

Fig. 20. PEEQT in the last increment obtained in the laboratory test (ARAMIS) (a) and in Abaqus (partial view) (b).

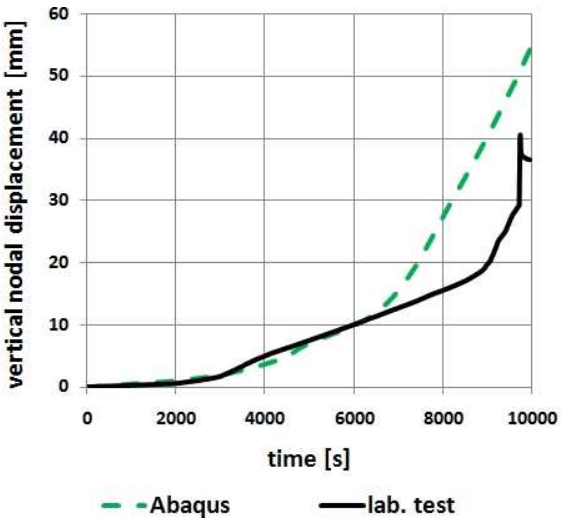

Fig. 21. The vertical nodal displacement in the middle of the beam.

5. Conclusions

The following conclusions can be drawn from the presented comparative analyses:

- at the presented stage of research, the numerical analysis satisfactorily reflected the behaviour of the element reinforced with composite rope; the results of vertical nodal displacement deviated

from each other after reaching 6000 s of the laboratory and numerical tests, and the response of the specimen in the laboratory test was stiffer,

- the crack pattern obtained from the numerical analyses satisfactorily overlapped with experimental studies, at least when considering crack pattern in the middle of the beam span; in FEM analysis carried out with Abaqus no diagonal cracks in the support zone occurred, but nevertheless the largest crack width occurred in the vertical crack,

- the image of the element deflection and damage in the case of numerical analysis deviated from the real state only in the final phase; the initial stiffness of the specimen both in laboratory tests and FEM analysis was almost identical,

- the authors suggested that the above-mentioned differences of laboratory and numerical tests in the last stage of loading might have also appeared because of the assumed full-bond constraint ("embedded region") of all model components in the FEM analysis (interaction and contact controls in Abaqus),

- in the further work, the authors are going to consider a more advanced model of the interface between steel, carbon fibre rope and concrete, and will also consider further calibration of some CDP model parameters in Abaqus (e.g., relaxation time, dilation angle, eccentricity parameter, post-peak behaviour of concrete in tension). A different plastic model of reinforcing steel, namely the elastic-plastic model with hardening instead of the elastic-ideally plastic model, should also be considered.

References

[1] T. Urban. *Strengthening of reinforced concrete structures with traditional methods* [in Polish: *Wzmacnianie konstrukcji żelbetowych metodami tradycyjnymi*]. WN PWN, 2015.

[2] M. Rajczyk, D. Jończyk. Strengthening of concrete structures with FRP fiber composites [in Polish: Wzmacnianie konstrukcji betonowych kompozytami włóknistymi FRP]. In: M. Major, *Zeszyty Naukowe Politechniki Częstochowskiej – Budownictwo*, **21**: 261–265. Wydawnictwo Politechniki Częstochowskiej, 2015.

[3] R. Kotynia. *Adhesion of composite reinforcement to concrete in reinforced concrete elements reinforced with composite materials* [in Polish: *Przyczepność zbrojenia kompozytowego do betonu w żelbetowych elementach wzmocnionych za pomocą materiałów kompozytowych*]. Zeszyt nr 16, Wydawnictwo Katedry Budownictwa Betonowego Wydziału Budownictwa i Architektury Politechniki Łódzkiej, Łódź, 2008.

[4] R. Kotynia. Analysis of reinforced concrete beams strengthened with near surface mounted FRP reinforcement. *Archives of Civil Engineering*, **2**: 305–317, 2006.

[5] R. Kotynia. *Strengthening of reinforced concrete beams using polymer composites* [in Polish: *Wzmacnianie żelbetowych belek na ścinanie za pomocą kompozytów polimerowych*]. Politechnika Łódzka – Zeszyty Naukowe Nr 1106, Rozprawy Naukowe, Łódź, 2011.

[6] M. Kałuża, T. Bartosik. Structure strengthening with materials based on carbon, glass and aramid fibers [in Polish: Wzmacnianie konstrukcji materiałami na bazie włókien węglowych, szklanych i aramidowych]. *Materiały Budowlane*, **2**: 36–38, 2007.

[7] Sika Wrap FX-50C product data sheet, https://gbr.sika.com/.

[8] P. Tworzewski, B. Goszczyńska. *An Application of an Optical Measuring System to Reinforced Concrete Beams Analysis*. In: Proceedings of 2016 Prognostics & System Health Management Conference – Chengdu (PHM-2016 Chengdu), China, 2016.

[9] J. Lubliner, J. Oliver, S. Oller, E. Oñate. A plastic-damage model for concrete. *International Journal of Solids Structures*, **25**(3): 299–326, 1989.

[10] J. Lee, G.L. Fenves. Plastic-damage model for cyclic loading of concrete structures. *Journal of Engineering Mechanics*, **124**(8): 892–900, 1998.

[11] Abaqus/CAE, User's guide, ver. 6-12.2, Dassault Systemes Simulia Corp., 2012.

[12] M. Szczecina, A. Winnicki. Selected aspects of computer modeling of reinforced concrete structures. *Archives of Civil Engineering*, **62**(1): 51–64, 2016.

[13] G. Devaut, J.L. Lions. *Inequalities in mechanics and physics*. Springer, Berlin Heidelberg, 1976.

[14] J. Szarliński, A. Winnicki, K. Podleś. *Concrete structures in plane states* [in Polish: *Konstrukcje z betonu w płaskich stanach*]. Politechnika Krakowska, Kraków, 2002.

[15] T. Jankowiak, T. Łodygowski. Identification of parameters of concrete damage plasticity constitutive model. *Foundations of Civil and Environmental Engineering*, **6**: 53–69, 2005.

[16] T. Jankowiak, T. Łodygowski. Quasi-static failure criteria for concrete. *Archives of Civil Engineering*, **56**(2): 123–154, 2010.

[17] T. Jankowiak. *Damage criteria of concrete under quasi-static and dynamic load* [in Polish: *Kryteria zniszczenia betonu poddanego obciążeniom quasi-statycznym i dynamicznym*]. Ph.D. thesis, Poznan University of Technology, 2010.

[18] A. Szwed, I. Kamińska. *On calibration of constitutive model parameters of concrete and laboratory tests serving that aim* [in Polish: *O kalibracji parametrów modelu konstytutywnego betonu i badaniach doświadczalnych temu służących*]. Chapter VIII in: E. Szmigiera, P. Łukowski, S. Jemioło [Eds]. Concrete and concrete structures – tests [in Polish: Beton i konstrukcje z betonu – badania], pp. 93–110. Warsaw University of Technology, Warsaw, 2015.

[19] EN1992-1-1 (2004) Eurocode 2 – Concrete structure – Part 1-1: General rules and rules for buildings.

[20] V. Červenka, L. Jendele, J. Červenka. *ATENA program documentation. Part 1 – Theory.* Červenka Consulting, Prague, 2012.